

Infrared Vision Systems for Emergency Vehicle Driver Assistance in Low-Visibility Conditions

M-Mahdi Naddaf-Sh^a, Andrew Lee^b, Kin Yen^a, Eemon Amini^c and Iman Soltani^{a,*}

^aDepartment of Mechanical and Aerospace Engineering, University of California - Davis, One Shields Ave, Davis, CA, 95616, USA

^bDepartment of Computer Science, University of California - Davis, 2063 Kemper Hall, Davis, CA, 95616, USA

^cThe Division of Research, Innovation and System Information, California Department of Transportation, 1120 N Street, Sacramento, CA, 95814, USA

ARTICLE INFO

Keywords:

Accident Prevention
Driver Safety
Emergency Vehicles
Infrared Camera
Low Visibility
Object Detection

ABSTRACT

This study investigates the potential of infrared (IR) camera technology to enhance driver safety for emergency vehicles operating in low-visibility conditions, particularly at night and in dense fog. Such environments significantly increase the risk of collisions, especially for tow trucks and snowplows that must remain operational in challenging conditions. Conventional driver assistance systems often struggle under these conditions due to limited visibility. In contrast, IR cameras, which detect the thermal signatures of obstacles, offer a promising alternative. The evaluation combines controlled laboratory experiments, real-world field tests, and surveys of emergency vehicle operators. In addition to assessing detection performance, the study examines the feasibility of retrofitting existing Department of Transportation (DoT) fleets with cost-effective IR-based driver assistance systems. Results underscore the utility of IR technology in enhancing driver awareness and provide data-driven recommendations for scalable deployment across legacy emergency vehicle fleets.


1. Introduction

Driving under low-visibility conditions presents significant safety challenges, particularly in areas with high traffic volumes and complex transportation networks Eklund, Rea and Bullough (1997). At night, in poor lighting conditions, or during foggy or severe weather, such as heavy rain or snow, visibility is significantly reduced, making it difficult for drivers to detect obstacles and react to sudden hazards. This issue is especially critical for heavy emergency vehicles, such as tow trucks and snowplows, which must continue operating under these conditions to clear roadways, assist stranded motorists or those involved in accidents, and ensure transportation routes remain open Dey, Mishra and Chowdhury (2015). Tow truck operators often need to navigate highways quickly to respond to collisions, accidental roadblocks, or breakdowns, while snowplow operators work to maintain accessibility in hazardous winter and icy conditions. Both types of emergency vehicles play a vital role in maintaining road safety, yet their ability to perform these tasks efficiently and safely is significantly hampered by limited visibility.

The reduced visibility endangers the public and the operators of these vehicles Peng, Abdel-Aty, Shi and Yu (2017). Especially in dense fog, the risk of collisions increases significantly, both for the emergency vehicles themselves and for other road users who may not see these large vehicles until it is too late Abdel-Aty, Ekram, Huang and Choi (2011); Hsiao, Chang and Simeonov (2018); Wang, Zhang, Feng, Yu and Wang (2021). Importantly, crashes occurring under fog or smoke conditions are significantly more severe than those under clear visibility, with higher rates of head-on and rear-end collisions, especially on high-speed, undivided, and unlit rural roads at night Abdel-Aty et al. (2011). Secondary collisions involving emergency vehicles, those that occur after an initial crash, are also a significant concern, particularly in the absence of comprehensive move-over laws Valente (2024); Karlaftis, Latoski, Richards and Sinha (1999). As climate change increases the frequency of extreme weather events, these challenges are likely to become even more prevalent Das, Barua and Hossain (2024), underscoring the need for advanced technologies to improve the safety and efficiency of emergency vehicle operations in low-visibility conditions.

* This research was funded by the California Department of Transportation (CALTRANS).

*Corresponding author

 isoltani@ucdavis.edu (I. Soltani)

ORCID(s): 0000-0001-9430-1522 (I. Soltani)

Most legacy emergency vehicles operated by DoTs are not equipped with modern advanced driver-assistance systems (ADAS). Even when such systems are present, their core components namely visible spectrum cameras and radars are primarily designed to enhance safety under standard driving conditions by detecting obstacles and issuing collision warnings Khan and Lee (2019). However, under low visibility scenarios like dark roadways, dense fog, heavy snowfall, or rain, these technologies face limitations Swief and El-Habrouk (2018). Standard cameras struggle to capture clear images in reduced visibility conditions Zakaria, Shapiai, Abd Ghani, Yassin, Ibrahim and Wahid (2023). Radar-based systems, though more robust in certain weather conditions, have limitations in detecting smaller or non-metallic objects, such as pedestrians or animals, that are commonly encountered during emergencies or in rural and unlit areas where wildlife crossings pose additional hazards Swief and El-Habrouk (2018); Ortiz, Sammarco, Costa and Detyniecki (2022). These limitations create critical gaps in the ability of these vehicles to navigate safely and respond effectively during emergency situations or snow-clearing operations.

IR cameras present a promising solution to the limitations faced by conventional ADAS technologies Farooq, Shariff, O'callaghan, Merla and Corcoran (2023); DiLorenzo and Yu (2023). Unlike visible spectrum cameras, IR cameras detect thermal radiation emitted by objects, including other vehicles, humans and animals, regardless of the lighting conditions. Additionally, the longer wavelength of thermal radiation makes it less susceptible to scattering from small particulates in fog, rain, or snow compared to visible light, allowing IR cameras to maintain a clearer view in such conditions Beier and Gemperlein (2004). Combining this characteristic with the latest advances in Machine Learning (ML)-based object detection Krišto, Ivacic-Kos and Pobar (2020) makes IR technology particularly well-suited for environments where visibility is severely compromised.

The objective of this research is to evaluate the potential of IR camera technology for driver assistance in low-visibility conditions, specifically in emergency response. This evaluation combines controlled laboratory experiments, real-world field testing, and feedback from emergency vehicle operators. In addition to assessing the performance of IR systems in challenging conditions, the study also explores the feasibility of retrofitting existing DoT fleets with cost-effective IR-based solutions. Given that many of these vehicles are aging and lack advanced ADAS, the successful integration of low-cost off-the-shelf IR technology could improve safety. The findings of this study aim to support policymakers and transportation agencies in making data-driven decisions regarding the large-scale adoption of IR cameras to improve both driver and public safety under low visibility conditions.

The paper hereafter is structured as follows: The Related Work section reviews existing research and technologies related to driver assistance systems in low-visibility environments, highlighting gaps that this study aims to address. In the Methodology, we describe the experimental setup and procedures used to evaluate the utility of commercial IR camera systems for driver assistance. The Experimental Results section presents the findings from these evaluations, including controlled experiments, real-world trials, emergency vehicle operators' feedback, and quantitative analysis. Finally, the Conclusions and Future Work section summarizes the implications of the results, and presents suggestions for further research.

2. Related Work

Previous research has demonstrated the effect of adverse weather conditions, including rain, fog, and snow, on the performance of sensors used in ADAS Zakaria et al. (2023); Pao, Li, Agelin-Chaab and Komar (2023); Rahman, Liu, Cheema, Chirila and Charlebois (2023). Visible spectrum camera-based systems are particularly susceptible to challenges in conditions such as dense fog, leading to reduced contrast and visibility, which hinders the sensors' ability to accurately detect and classify objects O'malley, Glavin and Jones (2011); Medina, Chitturi and Benekohal (2010). Radar systems, although more resilient in low-visibility conditions, can still experience degraded performance due to signal attenuation and scattering by precipitation, or reduced target reflectivity Hawkins and La Plant (1959). A similar limitation applies to LiDAR systems, whose performance can degrade due to signal scattering and absorption in rain, snow, or fog. However, LiDAR is rarely used in state-of-the-art ADAS, primarily due to its cost and integration challenges Kutila, Pyykönen, Holzhiiter, Colomb and Duthon (2018).

A study by Roh et al. Roh, Kim and Im (2020) demonstrated that when rain intensity exceeded 20 mm/hour, ADAS functionality, including obstacle detection and lane-keeping, was significantly compromised. Additionally, foggy conditions have been shown to impair both the visual and LiDAR systems of autonomous and assisted driving vehicles, causing delayed obstacle recognition and hazard response Aloufi, Alnori and Basuhail (2024); Peng, Jiang, Lu and Zou (2018).

There has been ongoing research to explore various techniques aimed at improving the performance of these sensors in adverse conditions. One common approach involves optimizing the configuration and operation of sensors to mitigate the negative effects of rain, fog, or snow. For instance, some studies have focused on dynamically adjusting camera settings, such as exposure time, aperture (F-number), and focus, to minimize the impact of raindrops, snowflakes, or reduced contrast on image quality Zang, Ding, Smith, Tyler, Rakotoarivelo and Kaafar (2019). Another strategy to enhance sensor performance involves integrating multiple sensor modalities to compensate for the limitations of individual sensors. Sensor fusion techniques, for example, combine data from cameras, radar, and LiDAR, enabling a more robust perception system Lundquist (2011). In these systems, radar's resilience to precipitation and fog complements the high resolution of cameras, while LiDAR provides precise depth information, improving object detection and classification in low-visibility conditions. Deep learning algorithms have also been applied to process sensor data more effectively Al-Haija, Gharaibeh and Odeh (2022). These methods, particularly convolutional neural networks (CNNs), can be trained to recognize and account for the effects of adverse weather, improving the accuracy of object detection and classification under challenging conditions Al-Haija et al. (2022). While these techniques have shown promise in enhancing the performance of conventional sensors, the fundamental physical limitations persist Ozarkar, Gely and Zhou (2022). No amount of post-processing or ML can fully compensate for the lack of information Zang et al. (2019).

Research has shown that IR cameras perform well in adverse conditions, particularly when detecting objects with heat signatures, such as pedestrians, animals, and active vehicles, making them well-suited for low-visibility scenarios Bhadoriya, Vegamoor and Rathinam (2022). Investigations conducted by commercial entities have also indicated that IR cameras can detect pedestrians at significantly greater distances than visible-spectrum cameras, even in complete darkness or dense fog FLIR-Systems (2025). Another focus has been on the integration of IR cameras with other sensor modalities, such as radar and LiDAR, to compensate for weaknesses in conventional systems Bhadoriya et al. (2022); Yeong, Velasco-Hernandez, Barry and Walsh (2021). However, the use of IR cameras is not without its challenges. Environmental factors like dirt, water droplets, and ice can accumulate on the camera lens, affecting image clarity. To address this, some researchers have proposed the use of advanced data processing techniques to minimize distortions and maintain detection accuracy Tumas, Serackis and Nowosielski (2021).

Despite extensive research on the potential of IR cameras, their real-world performance in driver assistance systems, especially for emergency vehicles, remains largely unexamined. Emergency vehicles face unique operational challenges, often navigating hazardous environments during rescue missions or road maintenance. These demanding conditions highlight the critical need for targeted evaluation. This study seeks to fill that gap.

3. Methodology

3.1. Evaluation Strategy

In this study, given the frequent occurrence of fog in Northern California, USA, we focus on evaluating the performance of IR cameras under both daytime and nighttime foggy conditions. Our research methodology consists of three main components: 1) Controlled laboratory experiments using synthetic fog, 2) On-road testing on a passenger vehicle, and 3) Deployment in emergency vehicles.

1. Laboratory Evaluation Using Synthetic Fog

To evaluate the performance of IR cameras in foggy conditions, we conducted controlled laboratory experiments using synthetic fog in an enclosed tent. An RGB camera and two commercially available IR cameras were tested to assess their ability to penetrate artificial fog. This setup enabled a direct qualitative comparison of image clarity and object detectability across the three cameras.

2. On-Road Testing

The RGB camera and the two commercially available IR cameras were installed on a test passenger vehicle (Fig. 1a) to assess their performance under clear and foggy conditions, including clear days, foggy days, clear nights, and foggy nights. The vehicle was driven through a range of real-world scenarios, capturing visual data from all three cameras simultaneously. The three cameras are securely mounted on a solid aluminum bar and affixed to the roof of the test vehicle. They are positioned side by side with minimal spacing to reduce discrepancies in their fields of view (FoVs). Residual differences in the captured images, arising from displacement or misalignment, sensor size, or lens characteristics, are corrected by cropping the images to a common, aligned FoV. To evaluate each camera's object detection capabilities, we manually annotated the images to establish ground truth for the objects present within the FoV. Additionally, we applied an ML-based object detection algorithm to each camera's output and compared their



Figure 1: (a) Test passenger vehicle with three cameras mounted on the roof. (b) Installed monitor inside the cabin of a tow truck. (c) Installed camera on the roof of a tow truck.

performance to the ground truth annotations. This analysis provided insights into the relative advantages and limitations of RGB and IR cameras in clearly capturing objects under different visibility conditions and in generating sufficient image quality for an ML-based method to reliably detect objects automatically.

3. Deployment in Emergency Vehicles To also assess the practical utility of IR cameras in real-world operations, we installed IR cameras in two emergency vehicles from the Caltrans District 4, covering areas such as the Bay Bridge, where fog is a frequent occurrence. To ensure ease of use, we adopted a simplified approach to integrating IR cameras into the vehicle system. The IR camera feed was displayed on an in-vehicle monitor, similar to front or backup cameras commonly found in modern vehicles, allowing drivers to refer to the system as needed in low-visibility conditions. Figures 1(b) and (c) show the placement of an IR camera and monitor on a Caltrans emergency vehicle. This design choice reduces the need for specialized training and facilitates cost-effective retrofitting of existing vehicle fleets. Given that many DoT emergency vehicles are aging and lack ADAS technologies, this approach offers an accessible safety enhancement. To further improve usability, an ML-based object detection system was integrated into the setup, overlaying bounding boxes around detected objects to draw the driver's attention to potential hazards. Vehicles retrofitted with the IR cameras were deployed in field conditions, and drivers were surveyed to assess their perception of the cameras' utility, particularly regarding situational awareness, safety improvements, and ease of use in low-visibility scenarios. Of the two IR camera models evaluated in this study, only one was installed in the emergency vehicles. The primary objective of this phase of the study was to assess the overall usefulness of IR camera technology rather than to compare the specific performance of the two IR camera models.

3.2. Selection of IR Camera

To identify the most suitable IR cameras for our study, we conducted a comprehensive review of commercially available options. The selection process was guided by the following key criteria:

1. Image Resolution and Quality: The camera must provide sufficient resolution and clarity to enable the drivers as well as the ML-based object detection system to accurately identify objects in low-visibility conditions.

2. Frame Rate: A high frame rate is essential for minimizing presentation delay, which directly impacts the driver's total reaction time in critical situations.

3. Connectivity: The camera should provide a live feed output to an in-vehicle monitor and an ML processing unit for real-time object detection. The latter is necessary only if the camera system lacks embedded object detection capabilities.

4. Cost: Given that large-scale adoption, whether as an Original Equipment Manufacturer (OEM) solution or a retrofit upgrade, is highly dependent on cost-effectiveness, cost was another factor in the selection process.

Following a comprehensive search, we selected two candidates: Teledyne from FLIR LLC Systems (2025) and Xsafe-II M6S from InfiRay Co. Ltd. InfiRay (2025).

FLIR Teledyne offers a resolution of 640x512 pixels and multiple models with various field-of-view options, ranging from 24° to 75°. The frame rate can be adjusted between 30 Hz and 60 Hz, providing real-time thermal video that can be fed directly into host systems via interfaces such as USB 2.0, Gigabit Multimedia Serial Link (GMSL), Ethernet, or Flat Panel Display Link (FPD-Link). This camera is well-suited for severe weather conditions due to its IP67-rated enclosure, which includes a heated window to prevent icing or fogging Systems (2025). However, the FLIR ADK lacks built-in object detection capabilities, meaning that automated detection or classification of objects would require the addition of processing hardware and custom software.

Our second selection, Xsafe-II M6S, similarly provides a resolution of 640x512 pixels but stands out due to its built-in AI-driven object detection module. The camera is capable of detecting and classifying pedestrians and vehicles, with real-time visual bounding box overlays around detected objects on the monitor feed. This added layer of ML processing can enhance driver awareness by automatically highlighting potential pre-defined obstacles, making the system readily usable without any customization. Like the FLIR, the Xsafe-II is also designed for severe weather, featuring IP67 and IP69K ratings for durability, as well as an automatic defrost function to maintain image clarity in low temperatures InfiRay (2025).

3.3. Custom ML-based Object Detection for Teledyne FLIR

The Xsafe-II features an onboard object detector that is pre-programmed into the device. In contrast, the FLIR camera outputs raw video data. While this may be seen as a limitation, it offers added flexibility to integrate and evaluate the latest object detection algorithms, given the rapid pace of progress in this domain. Also certain limitations of the object detection system in the Xsafe-II can be addressed through a custom ML implementation. Notably, a delay of approximately 150 ms was observed in the Xsafe-II output, which may impact its real-time usability. In contrast, the FLIR setup offers the flexibility to optimize the object detection pipeline to reduce latency.

To process the raw video from the FLIR camera for object detection, we adopted a deep learning-based method. To ensure optimal real-time performance, we focused on minimizing delay and maximizing the frame rate in our implementation of object detection. Since this system is intended for driver assistance, where reaction time is critical, any delay in processing effectively translates to a delayed driver response, potentially increasing the risk of accidents. An analogy can be drawn to the difference in reaction times between a sober driver and one with a marginally illegal Blood Alcohol Concentration (BAC). Studies indicate that, on average, a sober individual has a premotor reaction time of around 60-90 milliseconds shorter than a person with a BAC of slightly above the legal limit Hernández, Vogel-Sprott and Ke-Aznar (2007). This seemingly small difference can significantly impact a driver's ability to respond to sudden hazards. Applying this analogy to our system, if our object detection processing introduces an additional 100 milliseconds of delay, the driver's reaction time would be impaired to a level comparable to that of a legally intoxicated driver.

We selected NVIDIA Jetson as our ML edge computing platform due to its balance of computational power and energy efficiency for real-time processing. The FLIR camera is connected to the NVIDIA Jetson via a USB port, running YOLOv7 Wang, Bochkovski and Liao (2023) for object detection, selected for its lightweight architecture, ease of implementation, and potential for real-time, low-latency performance Wang et al. (2023). To assess the trade-off between cost and performance, we evaluated different versions of YOLOv7 on two Jetson platforms: the Nvidia Jetson Nano and the more powerful and more expensive Nvidia Jetson Orin Nano.

For training the object detection model for the IR cameras, we used the *Teledyne FLIR Thermal Dataset Systems* (2025), which provides fully annotated thermal and visible spectrum frames captured from over-the-hood driving scenes. The dataset contains a total of 26,442 fully annotated frames with 520,000 bounding box annotations across 15 different object categories. For our application, we selected the most relevant object classes: [person, bike, car, motor, bus, train, truck, dog, deer, other vehicle], while removing all unrelated categories to streamline training and improve detection accuracy. To enhance inference speed and meet real-time application requirements, we implemented the following techniques:

1. Model Scaling: The model was optimized to align with the computational constraints of the Jetson Nano devices by adjusting its structural parameters Wang et al. (2023). Specifically for the YOLOv7 model on the, we applied aggressive structural scaling by reducing both the number of convolutional layers and the number of channels in each layer. This resulted in a significantly shallower and narrower network with the parameter count reduced from approximately 37 million in the original YOLOv7 to 2.5 million in the scaled model. This drastic reduction

lowered the computational burden and memory usage of the model, which allowed faster and more efficient inference. Importantly, these improvements were achieved while preserving the original YOLOv7 design, simply at a smaller scale. This method alone led to an approximately 2.7x increase in inference speed on the Jetson Orin Nano with minimal compromise on performance.

2. Quantization: Post-training quantization was applied to reduce numerical precision in the model’s weights and activations, significantly lowering computational overhead while maintaining acceptable accuracy. This optimization helped improve processing efficiency without compromising detection reliability.

3. Inference Acceleration: We employed NVIDIA TensorRT NVIDIA (2024), a deep learning inference optimizer, to enhance throughput and reduce latency during model inference. TensorRT applies optimization techniques such as layer fusion and GPU-specific kernel tuning. It improved execution efficiency and significantly boosted the ML frame rate performance for the FLIR camera.

By integrating these optimizations, we substantially reduced computational complexity, enabling real-time processing at 62 Frames Per Second (FPS) on the Jetson Orin Nano despite its limited hardware resources. At this frame rate, surpassing the maximum capacity of the camera, virtually no additional delay was introduced into the camera’s video throughput, ensuring minimal latency in object detection.

Table 1 summarizes the processing speed results for both hardware platforms. We began our evaluation on the Jetson Nano due to its lower cost, with the goal of identifying a viable low-budget option. Starting with the YOLOv7-tiny model, which is a smaller and less powerful variant of YOLOv7, and its quantized/scaled version, we achieved a maximum frame rate of 24 FPS, which may still be acceptable for real-time applications. However, given this upper limit, testing larger models such as YOLOv7 on the Jetson Nano was deemed impractical, as the frame rate would have dropped below usable levels. Thus, on Jetson Nano, only the tiny variant of YOLO was considered feasible for deployment in resource-constrained scenarios.

To maintain the camera’s native 60 FPS throughput, we transitioned to the more powerful but costlier Jetson Orin Nano. On this platform, the quantized and scaled YOLOv7-tiny model achieved up to 90 FPS, comfortably exceeding our real-time processing target. This allowed us to evaluate more complex and powerful models like YOLOv7, which after optimization (quantization and scaling) reached a maximum of 62 FPS, sufficient to preserve the original frame rate of the input camera.

Table 1

Overall performance of object detector algorithm for FLIR. JN: Jetson Nano, JON: Jetson Orin Nano, TRT: TensorRT. w/ and w/o indicate with and without, respectively.

	YOLOv7-tiny	YOLOv7-tiny Quantized/Scaled	YOLOv7	YOLOv7 Quantized/Scaled
JN w/o TRT	7.5 FPS	13 FPS	-	-
JN w/ TRT	13 FPS	24 FPS	-	-
JON w/o TRT	-	47 FPS	12.5 FPS	34 FPS
JON w/ TRT	-	90 FPS	30 FPS	62 FPS

4. Experimental Results

4.1. Controlled Experiments: Synthetic Fog

To qualitatively compare performance under various levels of fog intensity, we conducted a series of controlled experiments inside a 10 × 20 ft tent equipped with an artificial fog generator. Both the Xsafe-II and FLIR camera systems demonstrated robust performance across varying visibility levels, from clear to heavily obscured conditions, consistently capturing clear visuals of objects and humans. In addition, the YOLOv7 object detection algorithm was tested, confirming its ability to detect objects in dense fog. In contrast, the RGB camera failed to produce usable imagery in heavy fog, significantly limiting its object detection capabilities. Sample shots extracted from the test are presented in Fig. 2.

4.2. Field Experiments on a Passenger Vehicle

We conducted a series of field experiments to quantitatively compare the performance of the three cameras described earlier. This evaluation was based on the detection performance of ML models, benchmarked against

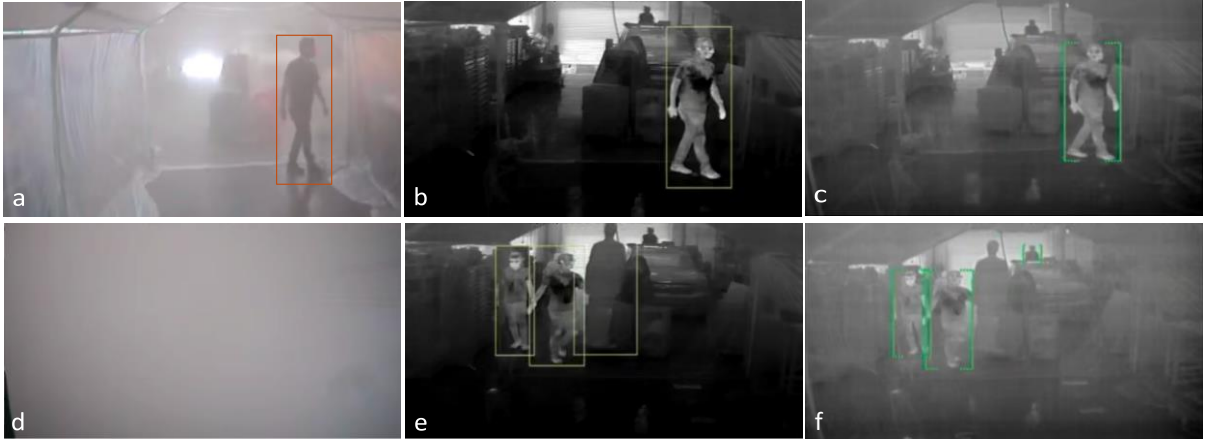


Figure 2: Sample frames from the synthetic fog experiment. Panels (a), (b), and (c) show RGB, Xsafe-II, and FLIR camera images, respectively, captured under light synthetic fog at the same timestamp. Panels (d), (e), and (f) present the corresponding images under dense synthetic fog, following the same camera order.

Table 2

RGB Camera and IR cameras object detector performance in clear day, late afternoon, clear night, foggy day, and foggy night conditions.

Weather Conditions	mAP@50%			F1 Score			Recall			IoU		
	RGB	FLIR	Xsafe-II	RGB	FLIR	Xsafe-II	RGB	FLIR	Xsafe-II	RGB	FLIR	Xsafe-II
Clear Day	0.8617	0.8103	0.7133	0.8369	0.9395	0.8749	0.8136	0.8859	0.7901	0.8331	0.8922	0.8912
Clear Night	0.7068	0.8001	0.7030	0.7044	0.9273	0.8676	0.7021	0.8861	0.7980	0.8088	0.8907	0.8882
Late Afternoon	0.7039	0.8924	0.7908	0.7376	0.9419	0.8759	0.7747	0.9183	0.8038	0.8166	0.8934	0.8933
Foggy Day	0.8583	0.7109	0.5419	0.6566	0.8085	0.7298	0.5317	0.7004	0.5855	0.8332	0.8912	0.8942
Foggy Night	0.6718	0.8076	0.6209	0.4737	0.8958	0.7567	0.3658	0.8330	0.6280	0.7821	0.8918	0.8920

ground truth annotations from simultaneous video footage recorded while driving a passenger vehicle under various environmental conditions (Fig. 1a). RGB data was included in the comparisons to highlight the contrast between visible and infrared spectrum capabilities under varying visibility conditions. For the FLIR IR camera, we used the YOLOv7 model described in Section 3.3. A separate YOLOv7 model, pre-trained on MS COCO Lin, Maire, Belongie, Hays, Perona, Ramanan, Dollár and Zitnick (2014), was fine-tuned on a subset of our annotated RGB footage. For the Xsafe-II system, we used the onboard object detection results provided by its embedded hardware. Detection performance across all environmental conditions is presented below.

Videos captured under various weather conditions were analyzed, with frames randomly selected and annotated as follows: 1500 frames (500 per camera) from foggy daytime conditions, 4500 frames (1500 per camera) from foggy nighttime conditions, 3000 frames (1000 per camera) from clear nighttime conditions, 1200 frames (400 per camera) from late afternoon conditions, and 4260 frames (1420 per camera) from clear day conditions. We used image timestamps to synchronize the frames from all three cameras. Table 2 presents the detection performance of all selected objects listed in 3.3 with respect to ground-truth human annotations. This table reports mAP@50, along with F1 score and recall calculated at a consistent confidence threshold of 0.7, which was kept fixed across all experiments. Intersection over Union (IoU) is also included to quantify the accuracy of object localization within the camera's field of view.

4.2.1. Clear Day and Clear Night

This data was collected to evaluate the performance of the cameras under both typical daytime and nighttime visibility conditions. During clear daytime, vehicle speed ranged from 0 to 70 MPH, and observations were made at various times of the day, including late morning, noon, and early afternoon. Clear daytime data includes sunny and cloudy conditions. For nighttime conditions, data were collected across the same range of vehicle speeds, capturing

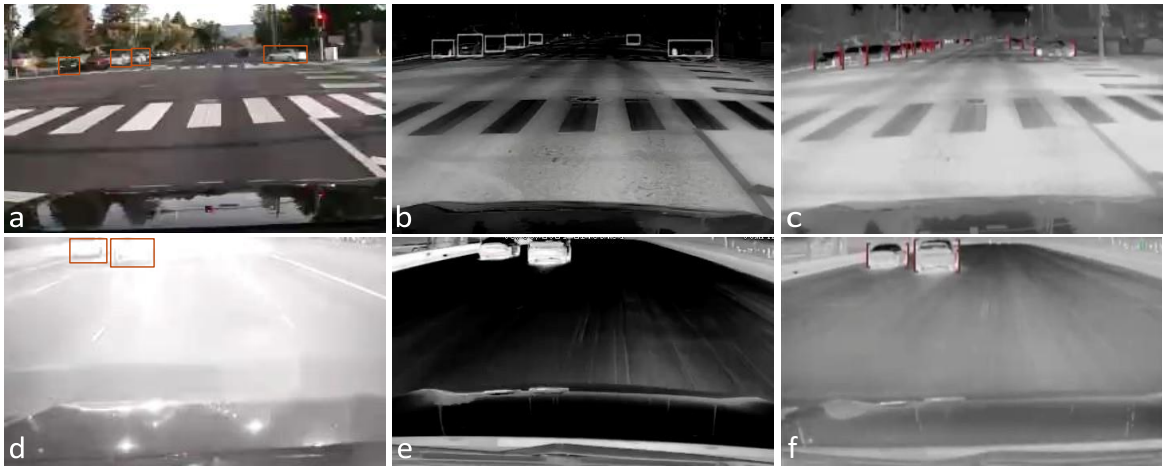


Figure 3: Example frames from clear day and clear night experiments. The clear day RGB, xSafe-II, and FLIR camera frame samples, at the same timestamps, are shown in (a), (b), and (c), respectively. The clear night samples in the same camera order are shown in (d), (e), and (f).

under different lighting environments, including areas with and without streetlights, as well as scenarios with and without oncoming traffic headlights.

As shown in Table 2, under clear day conditions, all three camera systems demonstrated relatively strong performance, benefiting from high visibility. The RGB camera achieved the highest mAP@50% (0.8617), reflecting precise object localization under visible light, which is consistent with the human driver’s view in ideal conditions. However, despite its slightly lower mAP (0.8103), the FLIR infrared camera outperformed the RGB camera in both F1 score (0.9395 vs. 0.8369) and recall (0.8859 vs. 0.8136), suggesting it was more consistent in detecting objects with fewer missed detections. The Xsafe-II camera showed the lowest performance among the three, with an mAP of 0.7133, an F1 score of 0.8749, and a recall of 0.7901. The IoU values were similar across all cameras, indicating that when objects were detected, the predicted bounding boxes were spatially accurate. Overall, while the RGB camera benefited from good visibility, the FLIR system still maintained robust performance, hinting at its reliability even in conditions that are already favorable for visible light cameras.

In clear night conditions, the performance gap between the FLIR infrared camera and the other two systems became more pronounced. The FLIR camera maintained strong performance with an mAP@50% of 0.8001, F1 score of 0.9273, and recall of 0.8861, demonstrating its ability to reliably detect objects under low light conditions. In contrast, the RGB camera’s performance dropped noticeably, with a lower mAP of 0.7068, F1 score of 0.7044, and recall of 0.7021. The Xsafe-II system achieved intermediate results, with an F1 score of 0.8676 and a recall of 0.7980. While this indicates some resilience to low-light conditions, its lower mAP (0.7030) may be attributed not only to hardware limitations but also to the efficiency and accuracy of its embedded ML model. IoU values were comparable across all cameras, suggesting similar spatial accuracy when detections occurred. Overall, these results emphasize the advantage of infrared imaging in nighttime driving scenarios. Example frames from clear day and clear night experiments are shown in Fig. 3.

4.2.2. Late Afternoon

Part of our tests were conducted during the late afternoon hours across the same speed profiles as clear day and night. This time window was chosen intentionally due to the unique visibility challenges it presents for drivers. In particular, direct sunlight near the horizon can lead to significant glare on the windshield and the camera lens, as well as high-contrast shadows that obscure objects in the environment. These conditions differ from those typically encountered during clear midday hours, when ambient lighting is more uniform and visibility is generally high. By including late afternoon scenarios in our testing, we aimed to evaluate the performance of the system under more challenging yet commonly encountered real-world conditions.

As seen on the third row of Table 2, during late afternoon conditions, the FLIR infrared camera again demonstrated a clear advantage, achieving the highest scores across all key metrics: mAP@50% of 0.8924, F1 score of 0.9419, and



Figure 4: Example frames from the late afternoon dataset at two timestamps (top and bottom rows), captured using three different cameras. From left to right: RGB, Xsafe-II, and FLIR camera views, respectively.

recall of 0.9183. The RGB camera showed the lowest performance among the three cameras with an mAP of 0.7039, F1 score of 0.7376, and recall of 0.7747. The Xsafe-II system showed intermediate performance, with an F1 score of 0.8759, a recall of 0.8038, and an mAP of 0.7908 all lagging behind FLIR but superior to RGB. These findings underscore the late afternoon as a realistic condition where IR-based systems, like FLIR, offer superior detection reliability. Fig. 4 shows examples of sun glare and high contrast shadow from the late afternoon data.

4.2.3. Foggy Day

This data was collected to assess the performance of camera systems in daytime foggy weather conditions. Vehicle speed varied from 0 to 55 MPH. In foggy day conditions, the performance differences between the cameras became a bit more evident. Sample images appeared blurry, and with the intensification of fog, detecting objects within the frame became unfeasible. Water droplets formed on the camera lenses, a consequence of the cameras being mounted externally on the vehicle and exposed to fog and humidity. The RGB camera achieved the highest mAP@50% of 0.8583. However, its F1 score (0.6566) and recall (0.5317) were substantially lower, suggesting it missed a significant number of objects due to the reduced visibility and low contrast typical of fog. In contrast, the FLIR infrared camera achieved a lower mAP (0.7109), but notably higher F1 score (0.8085) and recall (0.7004), reflecting its greater consistency in detecting objects in foggy environments. The lower mAP for FLIR, despite better recall, may reflect a higher rate of marginal detections that did not meet the IoU threshold. The Xsafe-II system showed the weakest performance, with all metrics, mAP, F1 score, and recall, falling to 0.5419, 0.7298, and 0.5855, respectively, likely due to both challenging conditions and limitations of its embedded detection model. Overall, these results suggest that the perceived advantages of IR cameras during daytime and under moderate fog conditions, consistent with our field experience (Fig. 2(a, b, c)), may not be as clear-cut. In our on-road driving experiments, we primarily encountered intermediate levels of fog, where IR cameras did not show a decisive advantage over RGB. However, as discussed earlier, controlled experiments under synthetic fog confirmed that under extremely dense fog, IR cameras clearly outperform RGB (Fig. 2(d, e, f)). A few examples of the foggy daytime conditions are shown in Fig. 5. As illustrated in the bottom row, under moderate fog and daylight conditions, condensation on the camera lens appears to pose a more significant challenge than the fog itself. However, this issue is not relevant to the driver's visibility inside the vehicle.

4.2.4. Foggy Night

This dataset was collected to evaluate the performance of camera systems in foggy weather conditions and at nighttime. Vehicle speeds were recorded, ranging from 0 to 50 MPH. Foggy night conditions posed the most challenging visibility scenario, combining low ambient light with low contrast due to fog. In this environment, the FLIR infrared camera clearly outperformed the other systems, achieving the highest F1 score (0.8958) and recall (0.8330), along with a solid mAP@50% of 0.8076. These results demonstrate FLIR's strong ability to consistently detect objects even in the most degraded visual conditions. The RGB camera, by contrast, showed a significant drop



Figure 5: Example frames from foggy daytime conditions at two different timestamps (top and bottom rows). From left to right, the images are captured by the RGB, Xsafe-II, and FLIR cameras, respectively.



Figure 6: Example frames from foggy nighttime conditions at two different timestamps (top and bottom rows). From left to right, the images are captured by the RGB, Xsafe-II, and FLIR cameras, respectively.

in performance, with an F1 score of just 0.4737 and recall of 0.3658, reflecting its limited capability to detect objects when both lighting and visibility are poor. The Xsafe-II camera performed better than the RGB camera but still lagged behind FLIR, with an F1 score of 0.7567 and a recall of 0.6280. Example frames from foggy nighttime conditions are shown in Fig. 6.

4.3. Feedback of Emergency Vehicle Drivers

A survey was conducted among tow truck drivers (San Francisco area, California, USA) to evaluate the performance and usability of the system across various conditions, as reported by eight operators. The survey included questions about usability, as well as ratings for overall satisfaction, safety improvement, display quality, and system reliability.

Operators rated the system relatively high for usability at clear night and during fog, with both conditions receiving an average score of 3.62 out of 5. Usability in the rain received slightly lower ratings, averaging 3.2 out of 5. Overall satisfaction with the system averaged 3.25 on a 5-point scale. Operators found the system effective in low-visibility conditions. However, screen lighting emerged as a common concern, primarily due to the lack of an auto-brightness feature. Survey responses indicated that, despite this limitation, the system is regarded as a useful safety aid. In response to driver feedback, the latest implementation now includes automatic brightness adjustment. Given that the initial

deployment focused on demonstrating overall utility, it was not expected to resolve all potential issues. With its value now established, the system presents clear opportunities for further improvement.

5. Conclusions and Future Work

This study demonstrates the potential of IR camera systems as a valuable component of driver assistance technologies for emergency and maintenance vehicles. Both controlled and real-world evaluations confirm that IR cameras can reliably detect obstacles under low visibility conditions, offering a meaningful safety enhancement. The findings also underscore the feasibility of retrofitting commercial off-the-shelf IR cameras into existing vehicle fleets. Their compatibility with current fleet architectures and the relatively low integration cost make them a practical and scalable solution for transportation agencies seeking to improve safety without extensive system overhauls. Another key insight from this work relates to the rapid advancements in deep learning and object detection technologies. Rather than relying solely on embedded ML within IR cameras, utilizing higher-quality cameras with external processing pipelines may offer greater flexibility. This decoupled approach allows for ongoing algorithmic improvements and optimization of processing throughput, reducing latency and boosting performance. Future research should explore large-scale deployment of IR camera systems across diverse operational environments to validate these results at scale and assess their impact on metrics such as collision avoidance and response times. Expanding the training dataset and retraining the object detection models with richer, more representative data could further improve detection accuracy. In parallel, efforts to refine the user experience are critical. Enhancements such as improved display quality or alternatives like auditory feedback or direct emergency braking interventions without a visual interface should be explored to maximize the effectiveness and usability of the system.

References

- Abdel-Aty, M., Ekram, A.A., Huang, H., Choi, K., 2011. A study on crashes related to visibility obstruction due to fog and smoke. *Accident Analysis and Prevention* 43, 1730–1737.
- Al-Haija, Q.A., Gharaibeh, M., Odeh, A., 2022. Detection in adverse weather conditions for autonomous vehicles via deep learning. *Ai* 3, 303–317.
- Aloufi, N., Alnori, A., Basuhail, A., 2024. Enhancing autonomous vehicle perception in adverse weather: A multi objectives model for integrated weather classification and object detection. *Electronics* 13, 3063.
- Beier, K., Gemperlein, H., 2004. Simulation of infrared detection range at fog conditions for enhanced vision systems in civil aviation. *Aerospace Science and Technology* 8, 63–71.
- Bhadoriya, A.S., Vegamoor, V., Rathinam, S., 2022. Vehicle detection and tracking using thermal cameras in adverse visibility conditions. *Sensors* 22, 4567.
- Das, S., Barua, S., Hossain, A., 2024. Unraveling the complex relationship between weather conditions and traffic safety. *Journal of Transportation Safety & Security*, 1–40.
- Dey, K.C., Mishra, A., Chowdhury, M., 2015. Potential of intelligent transportation systems in mitigating adverse weather impacts on road mobility: A review. *IEEE Transactions on Intelligent Transportation Systems* 16, 1107–1119. doi:10.1109/TITS.2014.2371455.
- DiLorenzo, T., Yu, X., 2023. Use of ice detection sensors for improving winter road safety. *Accident Analysis and Prevention* 191, 107197. URL: <https://www.sciencedirect.com/science/article/pii/S0001457523002440>, doi:https://doi.org/10.1016/j.aap.2023.107197.
- Eklund, N.H., Rea, M.S., Bullough, J., 1997. Survey of snowplow operators about forward lighting and visibility during nighttime operations. *Transportation research record* 1585, 25–29.
- Farooq, M.A., Shariff, W., O’callaghan, D., Merla, A., Corcoran, P., 2023. On the role of thermal imaging in automotive applications: A critical review. *IEEE Access* 11, 25152–25173.
- FLIR-Systems, 2025. Flir thermal for adas and av. https://www.flir.com/globalassets/email-assets/pdf/flir_thermal_for_adas_and_av.pdf. Accessed: 2025-02-19.
- Hawkins, H., La Plant, O., 1959. Radar performance degradation in fog and rain. *IRE Transactions on Aeronautical and Navigational Electronics*, 26–30.
- Hernández, O.H., Vogel-Sprott, M., Ke-Aznar, V.I., 2007. Alcohol impairs the cognitive component of reaction time to an omitted stimulus: A replication and an extension*. *Journal of Studies on Alcohol and Drugs* 68, 276–281. PMID: 17286346.
- Hsiao, H., Chang, J., Simeonov, P., 2018. Preventing emergency vehicle crashes: Status and challenges of human factors issues. *Human Factors* 60, 1048–1072.
- Infray, 2025. How to effectively improve the safety of car driving. <https://www.infray.com/how-to-effectively-improve-the-safety-of-car-driving.html>. Accessed: 2025-02-19.
- Karlaftis, M.G., Latoski, S.P., Richards, N.J., Sinha, K.C., 1999. Its impacts on safety and traffic management: an investigation of secondary crash causes. *Journal of Intelligent Transportation Systems* 5, 39–52.
- Khan, M.Q., Lee, S., 2019. A comprehensive survey of driving monitoring and assistance systems. *Sensors* 19, 2574.
- Krišto, M., Ivacic-Kos, M., Pobar, M., 2020. Thermal object detection in difficult weather conditions using yolo. *IEEE access* 8, 125459–125476.

- Kutla, M., Pyyk  n, P., Holz  ter, H., Colomb, M., Duthon, P., 2018. Automotive lidar performance verification in fog and rain, in: 2018 21st International Conference on Intelligent Transportation Systems (ITSC), IEEE. pp. 1695–1701.
- Lin, T.Y., Maire, M., Belongie, S., Hays, J., Perona, P., Ramanan, D., Doll  r, P., Zitnick, C.L., 2014. Microsoft coco: Common objects in context, in: Computer vision–ECCV 2014: 13th European conference, zurich, Switzerland, September 6–12, 2014, proceedings, part v 13, Springer. pp. 740–755.
- Lundquist, C., 2011. Sensor fusion for automotive applications. Link  pings Universitet (Sweden).
- Medina, J., Chitturi, M., Benekohal, R., 2010. Effects of fog, snow, and rain on video detection systems at intersections. *Transportation Letters* 2, 1–12.
- NVIDIA, 2024. TensorRT. <https://github.com/NVIDIA/TensorRT>. Accessed: 2025-04-12.
- O  malley, R., Glavin, M., Jones, E., 2011. Vision-based detection and tracking of vehicles to the rear with perspective correction in low-light conditions. *IET Intelligent Transport Systems* 5, 1–10.
- Ortiz, F.M., Sammarco, M., Costa, L.H.M., Detyniecki, M., 2022. Applications and services using vehicular exteroceptive sensors: A survey. *IEEE Transactions on Intelligent Vehicles* 8, 949–969.
- Ozarkar, S., Gely, S., Zhou, K., 2022. Physics-based simulation solutions for testing performance of sensors and perception algorithm under adverse weather conditions. *SAE International Journal of Connected and Automated Vehicles* 5, 297–312.
- Pao, W.Y., Li, L., Agelin-Chaab, M., Komar, J., 2023. Drive-thru climate tunnel: A proposed method to study adas performance in adverse weather. Technical Report. SAE Technical Paper.
- Peng, Y., Abdel-Aty, M., Shi, Q., Yu, R., 2017. Assessing the impact of reduced visibility on traffic crash risk using microscopic data and surrogate safety measures. *Transportation research part C: emerging technologies* 74, 295–305.
- Peng, Y., Jiang, Y., Lu, J., Zou, Y., 2018. Examining the effect of adverse weather on road transportation using weather and traffic sensors. *PLoS one* 13, e0205409.
- Rahman, T., Liu, A., Cheema, D., Chirila, V., Charlebois, D., 2023. Adas reliability against weather conditions: Quantification of performance robustness, in: 27th International Technical Conference on the Enhanced Safety of Vehicles (ESV) National Highway Traffic Safety Administration.
- Roh, C.G., Kim, J., Im, I.J., 2020. Analysis of impact of rain conditions on adas. *Sensors* 20, 6720.
- Swief, A., El-Habrouk, M., 2018. A survey of automotive driving assistance systems technologies, in: 2018 International Conference on Artificial Intelligence and Data Processing (IDAP), IEEE. pp. 1–12.
- Systems, F., 2025. Adas dataset form. <https://www.flir.com/oem/adas/adas-dataset-form/>. Accessed: 2025-02-19.
- Tumas, P., Serackis, A., Nowosielski, A., 2021. Augmentation of severe weather impact to far-infrared sensor images to improve pedestrian detection system. *Electronics* 10, 934.
- Valente, J.T., 2024. From crash to care: A road towards improved safety and efficiency of emergency medical response .
- Wang, C.Y., Bochkovskiy, A., Liao, H.Y.M., 2023. Yolov7: Trainable bag-of-freebies sets new state-of-the-art for real-time object detectors, in: Proceedings of the IEEE/CVF conference on computer vision and pattern recognition, pp. 7464–7475.
- Wang, K., Zhang, W., Feng, Z., Yu, H., Wang, C., 2021. Reasonable driving speed limits based on recognition time in a dynamic low-visibility environment related to fog—a driving simulator study. *Accident Analysis and Prevention* 154, 106060.
- Yeong, D.J., Velasco-Hernandez, G., Barry, J., Walsh, J., 2021. Sensor and sensor fusion technology in autonomous vehicles: A review. *Sensors* 21.
- Zakaria, N.J., Shapiai, M.I., Abd Ghani, R., Yassin, M.N.M., Ibrahim, M.Z., Wahid, N., 2023. Lane detection in autonomous vehicles: A systematic review. *IEEE access* 11, 3729–3765.
- Zang, S., Ding, M., Smith, D., Tyler, P., Rakotoarivelo, T., Kaafar, M.A., 2019. The impact of adverse weather conditions on autonomous vehicles: How rain, snow, fog, and hail affect the performance of a self-driving car. *IEEE vehicular technology magazine* 14, 103–111.